

MATHEMATICAL MODEL AND SIMULATION OF FREE BALLOON LIFTOFF IN THE PRESENCE OF SURFACE WINDS

Nihad E. DAIDZIC^{1, 2*}

¹AAR Aerospace Consulting, LLC, Saint Peter, MN 56082, USA

²Minnesota State University, Mankato, MN 56001, USA

Received 1 March 2021; accepted 28 July 2021

Abstract. A mathematical model of free balloon launches in windy conditions is based on the conservation of the linear momentum in horizontal and vertical axes. Linear momentum conservation equations are represented by a set of four non-linear first-order ODEs. Some ODEs were solved analytically, while the nonlinear Riccati ODE with variable coefficients for the vertical acceleration was solved using numerical ODE solvers. Transient aerodynamic lift and horizontal drag are caused by the slip flow over the balloon envelope. It takes free balloon ten half times to reach 90.9% of the wind velocity in a step function response. A launch condition was developed in terms of the minimum required envelope temperature for which the net aerostatic lift overcomes inert weight of a balloon. Perturbation analysis was used to explore changes in the net aerostatic lift. Simulations were performed to cases with and without envelope distortion and enhanced cooling due to forced convection. Since all balloon takeoffs are performed downwind, obstacle clearance becomes an issue due to rapid loss of aerodynamic lift. Balloons may stop climbing and even start descending shortly after liftoff despite intense heating representing real hazard.

Keywords: aerostatic lift, slip flow, transient aerodynamic lift, transient aerodynamic drag, envelope distortion, enhanced envelope cooling, numerical ODE solvers.

Introduction

In respect to Federal Aviation Administration (FAA) pilot certification standards (US Department of Transportation, Federal Aviation Administration, 1996b, 1997), free balloon class belongs to the Lighter-than-Air (LTA) category as the sustained flight is based on the buoyancy or *Archimedes'* displacement principle. Balloons are further divided into hot-air balloons (LBH) or *Montgolfière*, gas balloons (LBG) or *Charlière*, and hybrid balloons or *Rozieres* utilizing both concepts of lighter-than air lifting gases and heated air. There is no specific pilot certification for hybrid free balloons. Airships (excluding thermal airships) are the other LTA class within the FAA pilot certification standards. A summary of FAA LTA classes including FAI sub-classification is given in Table 1.

Balloons find many applications in aviation and related fields. From gas balloons used for atmospheric sounding to free (untethered) manned hot-air balloons used for personal, sight-seeing, and adventure flights. However, the commercial segment of LTA aircraft is miniscule compared to Heavier-than-Air (HTA) aircraft, such as, airplanes and helicopters operations (Daidzic, 2021). For that reason, much less research has been conducted in LTA aircraft design, performance, and operations. Although, a relatively simple (in terms of control, required instrumentation, and equipment) and very safe aircraft, an LBH flight is by no means devoid of potential hazards. One of the most common causes of incidents and accidents in hot-air ballooning is the takeoff (launch, liftoff) with moderate to strong surface winds,

Table 1. FAA classes of LTA category pilot certifications and FAI free balloons (Class A) and Airship (Class B) classifications

Hot-Air Balloons (LBH)	Gas Balloons (LBG)	Hybrid (currently no specific FAA pilot certification standards)	Airship
FAI AX-1 to AX-15	FAI AA-1 to AA-15	FAI AM-1 to AM-15	FAI BA, BX, BM, BT 1-10

*Corresponding author. E-mails: nihad.daidzic@aaraerospacecon.com; nihad.daidzic@mnsu.edu

low-level wind-shears, or lifting off from a sheltered place protected by upwind barriers. Since LBHs have no independent propulsion system(s) it seeks the condition of zero relative speed with the moving ambient air mass. However, any time a balloon experiences change in atmospheric wind over the envelope height a relative air motion over the envelope top develops causing transient aerodynamic (dynamic) lift. Such lift is often called “false or uncommanded lift” in ballooning jargon (US Department of Transportation, Federal Aviation Administration, 1982, 2008). But there is nothing false about it. It is real and at may support or even oppose (“false heavy”) the main source of lift – aerostatic buoyancy. The real problem exists during balloon launches with substantial winds at envelope heights. Every balloon takeoff is downwind. A large part of the aerodynamic (dynamic) lift will be lost soon after liftoff causing the balloon to start descending or continue at reduced climb-gradients with possible undesired touchdown or, worse, hitting obstacles during the initial climb. Simple rule-of-thumb is used to estimate takeoff distance over an obstacle in the presence of surface winds (US Department of Transportation, Federal Aviation Administration, 1996a). Especially dangerous is the situation of balloons colliding with the high-voltage powerlines (US Department of Transportation, Federal Aviation Administration, 1981). A typical LBH has very large mass and thermal inertia and it may take relatively long time before it responds positively to frantic heat inputs. Surface winds of more than 12–15 knots (6–7.5 m/s) would result in very challenging takeoffs and are normally not recommended. Tethered balloons are typically limited to maximum 8–10 knots winds as they are continuously exposed to slip flow and powerful aerodynamic forces on large envelopes. On the other hand, airships are in relative motion with the surrounding air and experience continuously both aerostatic and aerodynamic lift. Modern airships have thrust-vectoring capabilities using swiveling propulsion units, providing them with great maneuvering capabilities (Khoury & Gillett, 1999; Taylor, 2014).

An illustration of free balloon launch from sheltered position and strong surface winds is shown in Figure 1.

Deceived by apparently sufficient total lift, a balloon lifts off while being accelerated horizontally over the ground. A balloon pilot (aeronaut) has no way of judging how much of the total lift is the “false” or transient aerodynamic lift and how much is the “true” or the net aerostatic lift. Hence, rapid loss of the transient aerodynamic lift causes descent and later diminished climb. Even a fast succession of long burns may not be sufficient to restore the positive net static buoyancy rapidly enough to safely overfly obstacle(s).

The main goal of this article is to develop a mathematical model of free balloon launch with moderate to strong surface winds, windshear, and wind gradients. A 2nd Law of classical mechanics is used to formulate equations of motion in the horizontal and vertical directions. Some of the resulting Ordinary Differential Equations (ODE) were solved analytically and other numerically. Various takeoff scenarios with varying winds at envelope height were simulated. The effect of envelope distortion and forced-convection cooling was also considered. The results of this study can be used to gain more insights into to physics of transient lift and development of best flying practices.

Unmanned LBGs (zero-pressure, super-pressure), LBHs and airships find many scientific and technical applications (Aaron et al., 2002; Cameron et al., 1999; Carlson & Horn, 1983; Das et al., 2003; Du et al., 2019; Kayhan & Hastaoglu, 2014; Kreider, 1975; Kreith & Kreider, 1974; Lally, 1971; Morris, 1975; Shi et al., 2009) and have been also considered for solar-system space exploration, such as in the atmospheres of Venus and Titan (Daidzic, 2014; Dorrington, 2013; Furfaro et al., 2008). While manned LBGs are somewhat rare in the USA (using Helium as lifting gas), they are more common in Europe and elsewhere (using H₂ gas). The analysis presented in this article can be applied to all manned and unmanned as well as free and tethered (moored) balloons, but the focus is primarily on manned free LBH launches. Airworthiness standards and certification of manned free balloons in the USA is under the jurisdiction of the FAA (US Department of Transportation, Federal Aviation Administration, 1999). Important

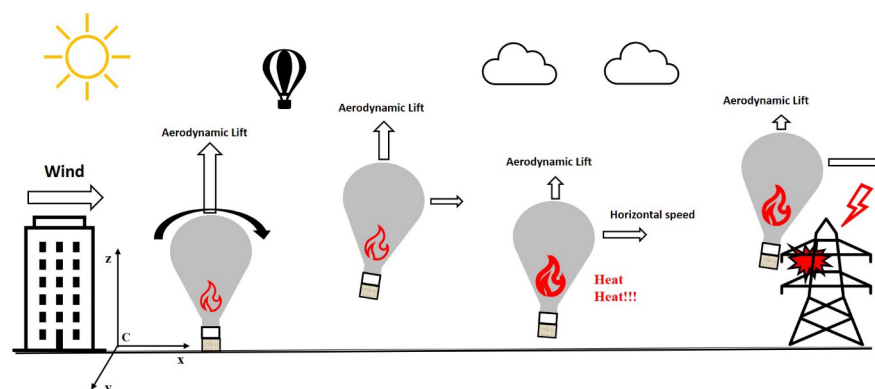


Figure 1. An illustration of balloon launch from sheltered place with significant horizontal wind (not to scale)

older treatment of basic ballooning theory and operations is given in Roth (1917). Good historical account of ballooning until the late 1970s is given in Jackson (1980).

The FAA pilot training material was the only source of information regarding the issue of “false” or aerodynamic lift. In Cameron (1980) and FAA (US Department of Transportation, Federal Aviation Administration, 1981, 2008), “false” lift is discussed and explained from the operator/pilot/aeronaut perspective only. The only place limited considerations of aerodynamic and thermal issues with the windshear, was found in the FAA (US Department of Transportation, Federal Aviation Administration, 1982). The problem of “false lift” was not addressed even in the classical treatments of free balloons by Kreider (1975), Kreith and Kreider (1974), Lally (1971), or Morris (1975). The heat transfer physics of hot-air balloons is discussed in Stefan (1979). Various principles of heat transfer applied to balloon flights are given in Kreith (1965). Jackson and Dichtl (1977) considered slip-flow and the half-time response to horizontal and vertical (thermal) wind shears. While the derivation by the authors is bit different from ours, the end results agree well. Jackson and Dichtl (1977) also present lucid model of the critical speed at which the slip-flow stagnation pressure starts distorting (dishing) balloon envelopes. The strength of the nylon and polyester envelope fabrics was measured by Stefan (1997) at various internal envelope temperatures and envelope’s age. Stefan (1997) used panel methods to compute potential flow pressure distribution around the envelope exterior for balloons exposed to vertical and horizontal slip flows. Intrigued by the, to the best of our knowledge, absence of scientific considerations of the free-balloons transient aerodynamic forces served as a strong motivator for this article. Transient slip flow and aerodynamic forces on balloon dynamics were addressed in this manner for the first time to the best of our knowledge.

1. Mathematical model of free balloon launch with arbitrary winds

The mathematical model developed here is based on a lumped-parameter differential model. It is assumed that the balloon is released from the ground with some excess of total effective lift accounting for the aerodynamic and the aerostatic lift. A topocentric, nearly-inertial frame of reference is fixed to a non-rotating flat-Earth approximation. Aerodynamic drag has quadratic speed dependence as the Reynolds numbers are sufficiently large. Lateral (acting horizontally) aerodynamic drag could also cause the lens-shaped deformation of the envelope (“dishing”) due to transient slip flow. Atmospheric winds normally increase with height, and both linear gradients and horizontal wind shears due to liftoffs from sheltered or protected places were assumed. No horizontal or vertical gusts were modeled although that would not present great difficulty.

Aerodynamic “false” lift appears due to relative motion of the atmospheric air over the envelope top. This can also happen when the balloon is ascending behind the sheltered place. In fact, the horizontal wind may also deform the envelope (lens-shape or “dish”) increasing its coefficient-of-drag, while simultaneously causing suction pressure over the envelope top. As the LBH is launched, it experiences horizontal drag and acceleration until the relative speed vanishes and its inertial ground speed equals the wind speed. That will also cause the aerodynamic lift to fade away rapidly due to the absence of relative motion in air. It may not be obvious to aeronauts how much of the total lift is in the form of this dynamic lift. Additionally, due to windshear, envelope may be distorted decreasing its volume and squeezing hot air out, the radiation thermal cooling of envelope is enhanced due to forced-convection heat transfer, and there may be cold air ingestion through the mouth. All these effects may cause significant reduction in aerostatic lift compounded by the rapid loss of aerodynamic lift.

The equations of motion in both horizontal and vertical directions are described using the Newton’s 2nd Law. Small balloon mass change during liftoff due to propane fuel consumption was neglected. It was assumed that no jettisonable ballast was released during launches. Sustained winds at the envelope top exist. Small changes in ambient air pressure and temperature during liftoff are neglected. Additionally, no net-change in envelope’s hot-air mass and thermal energy is assumed during short launch duration. The 2nd-order ODEs describing the unconstrained balloon motion with the lifting-gas mass and energy conservation equations and the equation of state for an ideal gas, yields:

$$\begin{aligned} M_i \frac{dv_x}{dt} &= \frac{1}{2} \rho_a (w - v_x)^2 C_{Dx} A_{ref} \\ M_i \frac{dv_z}{dt} &= g V_B (\rho_a - \rho_g) + \frac{1}{2} \rho_a (w - v_x)^2 C_L A_{ref} - \\ & m_B g - \frac{1}{2} \rho_a C_{Dz} A_{ref} |v_z| v_z \\ \frac{dm_g}{dt} &= 0 \quad \frac{d(m_g h_g)}{dt} = 0 \quad p_g = \rho_g R_g T_g. \end{aligned} \quad (1)$$

The inertial balloon mass M_i accounts for the inert mass m_B (envelope, basket, burners, venting and crown ropes, equipment, instrumentation, crew, ballast), internal lifting-gas mass m_g (hot air in this case) and the amount of environmental air m_a being affected and accelerated by a moving balloon. This inertial mass of ambient air being accelerated is accounted for by using the virtual mass coefficient C_{vm} (Das et al., 2003; Kayhan & Hastaoglu, 2014) with commonly:

$$M_i = m_{LBH} + m_B = (m_g + C_{vm} \rho_a V_B) + m_B \text{ and } C_{vm} \approx 0.25 - 0.5.$$

If the relative (slip) velocity between the steady horizontal wind (w) and the LBH groundspeed is defined as a difference between the steady wind speed and the horizontal LBH speed ($u = w - v_x$), then from Eq. (1):

$$\frac{dx}{dt} = w - u \quad \frac{du}{dt} + K_x(u) \cdot u^2 = 0. \quad (2)$$

$$\frac{dz}{dt} = v_z \quad \frac{dv_z}{dt} = g \left(\frac{\rho_a - \rho_g}{\rho_i} - \frac{\rho_B}{\rho_i} \right) + N(u) \cdot u^2 - \quad (3)$$

$$K_z(u, v_z) \cdot |v_z| v_z,$$

where: $\rho_i = M_i(u)/V_B(u)$, $\rho_B = m_B/V_B(u)$. The most general initial conditions (ICs) are: $x = x_0$, $u_0 = w - v_{x0}$, $z = z_0$, $v_z = v_{z0}$. Typically, the aerodynamic coefficients and geometric characteristics are slip-speed dependent:

$$K_x(u) = \frac{\rho_a C_{Dx}(u) A_{ref}(u)}{2 \cdot M_i}$$

$$K_z(u, v_z) = \frac{\rho_a C_{Dz}(u, v_z) A_{ref}(u)}{2 \cdot M_i} \quad (4)$$

$$N(u) = \frac{\rho_a C_L(u) A_{ref}(u)}{2 \cdot M_i}$$

$$A_{ref}(u) = \frac{D_e^2(u) \pi}{4} \quad V_B = V_B(u).$$

The auxiliary semi-empirical algebraic expressions were developed to model changes of the envelope volume and reference area (and equatorial diameter) due to windshear/gusts caused distortions (“dishing”), lateral and longitudinal drag coefficients C_{Dx} and C_{Dz} (McCormick, 1995) due to envelope distortions, and the reduction of the average hot-air temperature T_g due to enhanced (forced convection) cooling. Drag coefficients itself are slip velocity dependent. In these cases, the set of four nonlinear ODEs becomes strongly coupled with the numerical solutions being the only alternative. If there is no envelope distortion and temporary enhanced colling due to slip flow is neglected, the above coefficients become simple constants.

ODEs in Eqs. (2) and (3) with associated ICs represent Cauchy’s IVP. The coefficients K_x and K_z contain drag coefficients C_{Dx} and C_{Dz} of a balloon in lateral and vertical motions. While the first-order nonlinear ODE in Eqs. (2) can be solved by separation of variables, the same cannot be said of the Riccati-type ODE given in Eq. (3) (Abell & Braselton, 2010; Davis, 1962; Spiegel, 1981; Weber & Arfken, 2004; Zwillinger, 1992). Indeed, the first-order nonlinear ODE in Eq. (3) is the famous and fascinating Riccati equation with variable (time-dependent) coefficients and is generally extremely difficult to solve analytically requiring special methods and techniques (Nayfeh, 2004; Spiegel, 1981). That being beyond the scope of this article, the Riccati-type ODE will be integrated numerically using in-house developed ODE solvers.

The coefficient N in Eq. (4) contains the lift-coefficient (C_L) of the hemispherical envelope top. Sensitivity analysis was performed and estimated value of C_L was set at about 0.25. Panel methods (Anderson, 1991; Houghton & Carpenter, 1993; Moran, 2003) could be utilized in future to compute aerodynamic coefficients of the balloon envelope in slip flow. Alternatively, CFD analysis could be performed to estimate coefficients of lift and

drag. Such substantial effort is well beyond the scope of the present article. The free balloon launch starts when the sum of aerostatic and transient aerodynamic lift exceeds inert weight. After releasing the free balloon, it will start climbing and accelerating downwind. However, the aerodynamic lift will decline rapidly as balloon accelerates over the ground to achieve zero-slip flow. Therefore, the often called “false lift” is real, but the problem is that it is temporary, and the available net aerostatic lift may not be sufficient for required climb profile causing the balloon to start occasionally even losing height just as it is supposed to climb to clear obstacles. Unlike powered aircraft balloons always take off downwind. The required, but not necessarily safe, launch requirement for a balloon is:

$$g \left(\frac{\rho_a - \rho_g}{\rho_i} - \frac{\rho_B}{\rho_i} \right) + N w^2 > 0. \quad (5)$$

This positive net launch acceleration condition implies net positive vertical force resulting in positive liftoff due to aerostatic and aerodynamic lift. But this condition does not guarantee sustained climb once the balloon has lifted as the operator (aeronaut) may not be able to distinguish between the sustained aerostatic and transient aerodynamic lift. Aerodynamic (dynamic) lift will rapidly diminish soon after liftoff as a balloon accelerates downwind by reducing the slip speed between the moving air mass and the balloon’s inertial speed. If the aerostatic net lift alone does not exceed balloon’s inert weight, it may start descending while moving horizontally over the ground. That could be hazardous due to large inertia and sluggish response to heat inputs. Unfortunately, too many launch incidents and accidents have occurred under exactly these scenarios (Cameron, 1980; US Department of Transportation, Federal Aviation Administration, 1982).

The first-order nonlinear ODE for slip velocity in Eq. (2) can be solved by separation of variables assuming the drag coefficient K_x is independent of the slip speed resulting in:

$$u(t) = \frac{w}{1 + wK_x t} \Rightarrow v_x(t) = v_{x0} + w \left[1 - \frac{1}{1 + wK_x t} \right] \quad (6)$$

$$\frac{dv_x}{dt} = -\frac{du}{dt} = \frac{w^2 K_x}{(1 + wK_x t)^2}.$$

The horizontal distance free balloon covers during horizontal acceleration is decoupled from the vertical motion:

$$x(t) = \int (w - u) dt = x_0 + w \cdot t - \frac{1}{K_x} \ln(1 + wK_x t). \quad (7)$$

The first term in Eq. (7) is the wind-distance and the 2nd term is the slip-distance. The instantaneous climb angle is computed from the ratio of the vertical and the horizontal speeds. The time and horizontal distance required for the LBH to achieve half of the wind-speed is:

$$v_{x,50\%} = \frac{w}{2} \Rightarrow (HT)_{50\%} = \frac{1}{wK_x}$$

$$x_{50\%} = \frac{1}{K_x} [1 - \ln(2)] \approx \frac{0.307}{K_x}. \quad (8)$$

It is easily shown that a free balloon will reach about 91% of the wind speed after ten half-times in response to step slip speed input. Similar dynamics takes place as the balloon climbs through different wind layers. It takes time for the slip flow to vanish asymptotically. Similar analysis can be applied to vertical slip flows by encountering thermals as was shown in Jackson and Dichtl (1977). As the slip velocity and Reynolds number decrease, a turbulent slip flow may become laminar Stokes' (creeping) flow, and the drag equation becomes linearly dependent on the slip speed (Granger, 1995). Turbulent drag equation could be still used with the implication that the coefficient of drag will start rapidly increasing with lower Reynolds number, but such cases are largely unimportant for balloons. Remaining slip flow can only be detected by sophisticated instruments. Thus, balloons are rather accelerating sluggishly. Half times are inversely proportional to the lateral drag coefficient. The aerodynamic lift is practically always present during free balloon flight, but it is also weak and irrelevant for most cases. Numerical integration of Eq. (3) using simple, reliable, sufficiently accurate, and easily coded programs, such as, the predictor-corrector Heun's method or the modified-Euler, also known as the midpoint Runge-Kutta method, is implemented here (Abell & Braselton, 2010; Carnahan et al., 1969; Chapra & Canale, 2006; Press et al., 1992). The 2nd-order midpoint Runge-Kutta (RK2) method is particularly useful by computing the slope at the midpoint of the (time) interval and then applying midpoint slope at the starting point resulting in an iteration scheme more accurate than the basic (forward-time-difference) *Euler's* method. The ICs are used to start the marching-in-time process. The integration time interval was varied between 0.1 and 0.2 seconds to explore convergence and error propagation. Total takeoff time histories of up to 60 seconds were considered, thus keeping truncation and roundoff errors relatively small.

Interestingly, since the initial (launch) climb rates in manned free hot-air balloons are normally in the range of 100–300 fpm (0.5–1.5 m/s), the vertical accelerations are low (on the order of 0.05–0.1 m/s² or 10⁻² g), an approximate analytical solution of the vertical balloon speed and distance can be obtained by neglecting the aerodynamic drag in Eq. (3) due to vertical slip motion. Analytical integration for undistorted envelope and no-drag results in:

$$v_z(t) = v_{z0} + gt \left(\frac{\rho_a - \rho_g}{\rho_i} - \frac{\rho_B}{\rho_i} \right) + \quad (9)$$

$$\left(\frac{N}{K_x} \right) \left(w - \frac{w}{1 + wK_x t} \right); \quad \frac{N}{K_x} = \frac{C_L}{C_{Dx}};$$

$$z(t) = z_0 + \frac{gt^2}{2} \left(\frac{\rho_a - \rho_g}{\rho_i} - \frac{\rho_B}{\rho_i} \right) + \quad (10)$$

$$\left(\frac{N}{K_x} \right) \left(w \cdot t - \frac{1}{K_x} \ln |1 + wK_x t| \right).$$

The ratio (N/K_x) is essentially the aerodynamic efficiency of a balloon. A necessary, but not sufficient, condition for safe balloon launch requires that (Daidzic, 2021):

$$T_g > \frac{\rho_a T_a V_B}{\rho_a V_B - m_B R T_a} = \left(\frac{\rho_a}{\rho_a - \rho_B} \right) T_a. \quad (11)$$

This condition requires that the effective aerostatic lift exceeds balloon's inert weight. Condition given in Eq. (11) cannot address secondary effects due to surface winds, such as envelope augmented colling and shape distortions (volume reductions) resulting in additional loss of aerostatic lift. Furthermore, this condition does not guarantee obstacle clearance as the climbing balloon accelerates downwind. Safe thermal energy reserve is required to ensure positive buoyancy margins to enable required climb gradients in moderate to strong surface winds (e.g., more than 8–9 knots). The net aerostatic lift as a function of slip-speed is:

$$L_{static,eff}(u) = gV_B(u) \frac{\rho_a}{RT_a} \left[1 - \frac{T_a}{T_g(u)} \right]. \quad (12)$$

Utilizing the small linear perturbations theory around an arbitrary stationary point and utilizing the definition of the ambient air and lifting-gas super-heat functions (Daidzic, 2021), one obtains:

$$\frac{\Delta L_{eff}}{L_{eff}} = \frac{\Delta V_B}{V_B} + \frac{\Delta \rho_a}{\rho_a} - \frac{\Delta T_a}{T_a} \left(\frac{1}{\vartheta_g} \right)_0 + \frac{\Delta T_g}{T_g} \left(\frac{1}{\vartheta_a} \right)_0. \quad (13)$$

ISA Troposphere model is used for dry atmospheric air computations (Daidzic, 2015; Taylor, 2014).

2. Results and discussion

A 3,000 m³ 800 kg (inert weight) AX-9 LBH launch simulation is presented next. The entire balloon with the basket is about 20 m tall. Wind at the height of the envelope is steady at 11 knots (12.65 mph or 5.66 m/s). Standard pressure at 540 m (1,773 ft) is 950 hPa. DA (dry air) at 540 m PA and ambient 20 °C is 842 m (2,764 ft). Envelope equatorial diameter is 18 m. Estimated envelope's coefficient of lift (C_L) is 0.25. Assumed LBH longitudinal coefficient of drag is 0.5, while the lateral is 0.7. Average measured envelope temperature is 108 °C, resulting in a net aerostatic lift of 7,668 N. LBH inert weight is 7,845 N (excess of aerostatic lift is thus negative), while the initial aerodynamic lift with the 11-knot surface wind is 1,150 N (259 lb). The initial total lift of 8,818 N (1,982 lb) rapidly losses most of the dynamic lift component, resulting in negative excess of lift occurring (maximum 177 N) after only 12 seconds since airborne. Uniform wind speed, horizontal balloon speed, slip speed (left axis), vertical speed and acceleration (right axis) are all shown in Figure 2. The vertical speed has been integrated from the vertical acceleration ODE for the cases of no aerodynamic drag approximation and by numerically integrating full equations of motion using the simple Euler method and 2nd-order Runge-Kutta (RK2) numerical ODE solvers. The no-drag vertical dynamics clearly result in larger deviations, while the difference between the Euler and RK2 methods is reasonably small. The more accurate 4th-order Runge-Kutta (RK4) numerical solver resulted in indistinguishable improvement compared to RK2 solver.

The computed HT is 7.47 seconds, and the half-time distance is about 13 m. Even 60 seconds since the launch there is still some light slip-flow left (0.63 m/s or 1.2 knots). As Figure 3 shows, the maximum height reached after launch is about 15.3 m (50 ft) at about 37 seconds after and 133 m horizontally from the launch site after which the LBH starts descending due to significant loss of aerodynamic lift and net negative excess of lift. The minimum safe hot-air temperature is 110.66 °C indicating insufficient aerostatic lift for the safe launch. The analytical no-drag-approximation trajectory shows large deviations from the numerically integrated full model. While the difference is relatively small using numerical solvers, the RK2 solver returns more accurate results than accumulated error in two integrations using Euler’s method. The climb angle using RK2 solver was initially highest reaching about 17 angular degrees. As the decreasing climb angle reaches zero, the maximum height is reached.

Aerodynamic and aerostatic forces for undistorted envelope are shown in Figure 4. The aerodynamic lift decreases rapidly from 1,150 N to less than 200 N (45 lb) remaining after about 10 seconds since liftoff which can surprise aeronauts in the critical launch phase. Vertical drag shows change from climbing to descending flight at about 37th second. Due to quadratic nature, aerodynamic drag is always positive, but the drag vector may change direction. Although excess of lift becomes zero at about 12 seconds since launch, due to inertia the balloon continues climbing at progressively slower rates, until 37 seconds after liftoff it reaches maximum. This must be anticipated as adding heat at this moment may not suffice to arrest ensuing descent and possible ground contact.

Previous simulations have been performed without envelope distortion, and/or enhanced envelope cooling due to slip flow. Semi-empirical approach to envelope distortions affects the net aerostatic lift and the envelope’s lateral and longitudinal coefficient-of-drag and coefficient-of-lift. Linear dependance on the slip velocity is assumed. Linear modeling of the enhanced envelope colling due to slip flow was also implemented. Since the coupled ODE problem is nonlinear, numerical solution of ODEs was utilized. Thus, an RK2 ODE solver was used due to simplicity and

sufficient accuracy. The results for balloon horizontal and vertical speed and accelerations are shown in Figure 5.

Results account for envelope distortion due to slip flow. Compared to previous non-distorted case, increased coefficient of lateral drag increases horizontal acceleration and reduces half-times (HT is 6.77 seconds). It was assumed that balloon first lifted four meters (13 ft) undisturbed reaching vertical speed of 0.5 m/s (about 100 fpm) behind an obstacle after which it suddenly experienced sustained horizontal wind of 6.2 m/s (12 knots). The average hot air

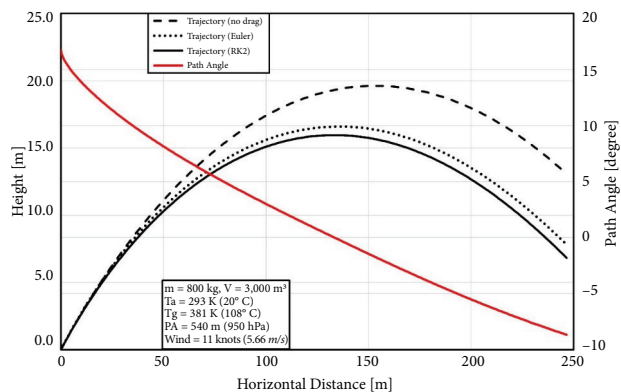


Figure 3. LBH launch horizontal and vertical speed histories with undistorted envelope

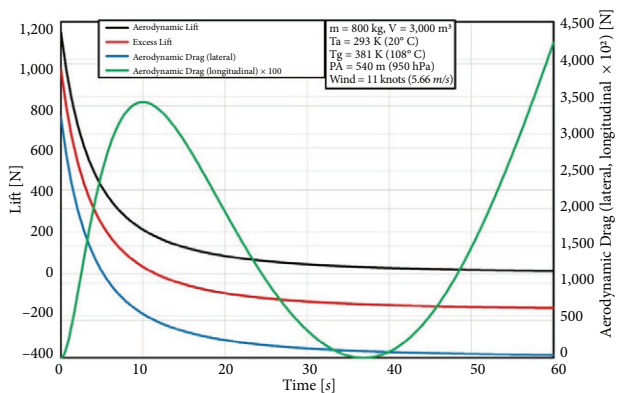


Figure 4. Aerodynamic lift, excess lift, and aerodynamic drag histories with undistorted envelope

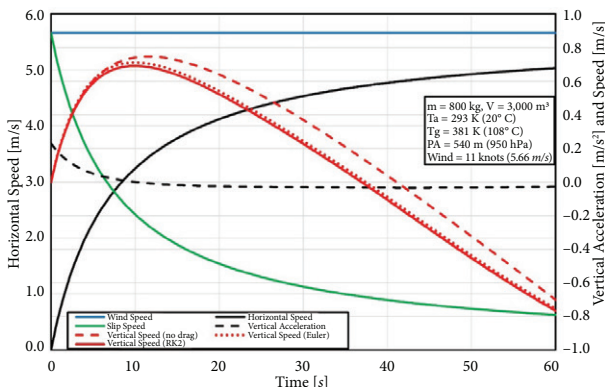


Figure 2. LBH launch at 11 knots surface winds with undistorted envelope

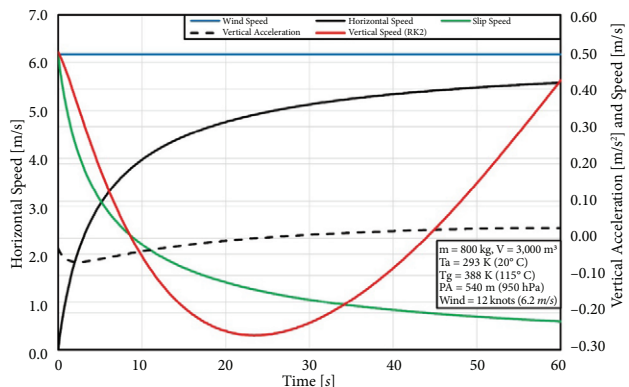


Figure 5. LBH launch simulation with distorted envelope

temperature is increased to 115 °C in this case to account for the loss of effective lift as it comes out of shelter. As the balloon experiences horizontal wind, dynamic lift develops which would normally increase performance.

Simultaneously, an envelope gets distorted with faster cooling taking place resulting initially in a net loss of lift and height despite transient aerodynamic lift. As the balloon accelerates, envelope distortions and enhanced cooling is decreasing restoring the aerostatic and net lift despite rapidly fading aerodynamic lift. Hence, the aerostatic lift is restored resulting in net increase of lift and a “yo-yo” trajectory profile with subsequent restored climb capabilities. However, a significant horizontal distance was covered, and the obstacle clearance downwind becomes doubtful. Trajectory and the path angle are shown in Figure 6. After 192 m the ground contact occurred with LBH rebounding. 60 seconds and almost 300 meters downwind, a balloon is essentially at the same height it was at the beginning of the launch. Time histories of aerodynamic and aerostatic forces acting on the balloon are shown in Figure 7.

Vigorous burner action is needed to restore loss of the aerostatic lift and quickly dissipating dynamic lift. After 10 seconds, the aerodynamic lift is only 175 N (39 lb). At the same instant, the lateral drag is less than 600 N (135 lb).

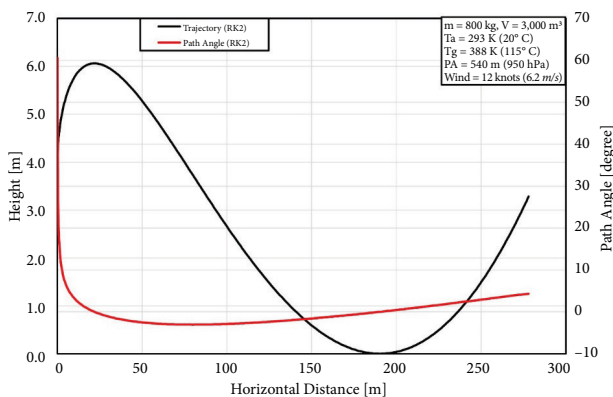


Figure 6. LBH launch horizontal and vertical speed histories with distorted envelope

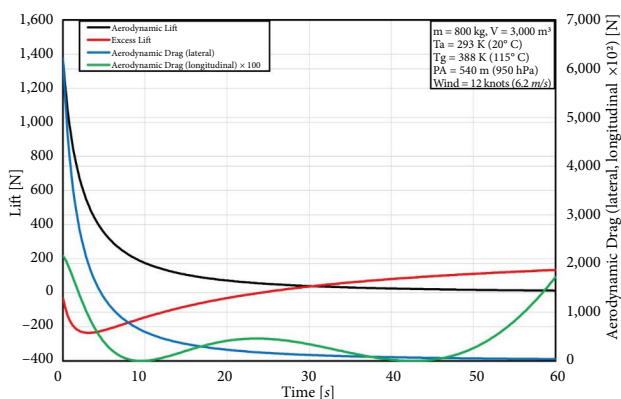


Figure 7. Aerodynamic lift, excess lift, and aerodynamic drag histories for distorted envelope

Excess lift, which becomes negative due to slip-flow induced envelope distortion is restored to positive value about 25 seconds after launch. Vertical and longitudinal drag is always opposing motion.

Balloon's large mass and thermal inertia causes slow and lagging response to thermal energy (burner) inputs which is especially critical in false-lift liftoff situations. For a fictitious AX-9 3,000 m³ (about 106,000 ft³) envelope with the internal representative hot-air temperature of 120 °C (393 K) and SL ISA conditions, the mass of lifting gas is about 2,695 kg and the heat energy content of hot-air is about 1.0697 GJ. The net heating (caloric) value of Propane (C₃H₈) is about 20,000 BTU/lb or 46.42 MJ/kg. A typical LBH system has two 3-MW (about 10 million BTU/hr heat rating) high-efficiency vaporizing burners rated at nominal operating propane vapor pressure at STP.

A 4-second single-burner burn will add about 12 MJ (about 3.33 kWh or 11,374 BTU) thermal energy to the envelope. Mass flow rate of liquid propane to generate 3-MW thermal power with the known effective propane heating value is about 0.065 kg/s. Liquid propane has density of about 500 kg/m³. Hence a twin-burner at maximum rated power of 6-MW operating continuously will consume an 85%-filled 10-gallon liquid propane tank in about 124 seconds of cumulative use (in 248 seconds of 3-MW single-burner use). Absent envelope cooling, a 4-second single-burner operation would increase envelope temperature by 4.4 °C (1.1 °C/second of burn time).

A 3,000 m³ natural-shape LBH envelope will have outside wetted surface area of about 1,400 m² (Morris, 1975). In the case of strong windshear an LBH will experience significant relative flow thus inducing the forced-convection heat transfer on the outside of the envelope and therefore the overall heat loss. For a uniform 100 °C temperature difference between the internal turbulent-mixed and vigorously recirculating hot-air and the outside environmental air and the overall heat transfer coefficient (neglected conduction resistance in the thin nylon envelope and envelope radiation heat transfer) of about 10 W/m²K, the specific heat flux becomes 1000 W/m² and the overall heat flux of 1.4 MW causing envelope cooling of about 0.5 °C/second. Jackson and Dichtl (1977) calculated the heat loss due to thermal radiation only (absence of free or forced convection) of about 0.21 °C/s, while their measurements in still air returned values of about 0.11 °C/s. Heat gains due to solar irradiation were not considered.

Our estimates reveal that during single-burner operation, the net envelope temperature increase in moderate windshear conditions is 0.6 °C/s. A 4-second single-burner standard burn will increase envelope's internal air temperature by 2.4 °C or (about 0.6% at 393 K) and increase the net aerostatic lift by about 1.8% (see Eq. 13). Therefore, intense heating utilizing all burners may be required to avoid settling back to the ground and/or to clear obstacles downwind. Strong windshear during takeoff may cause significant distortions and tilting of the envelope so that flames from burners may damage the vertical load tapes and envelope gores (“flame thrower effect”). This

must be avoided at all costs (Cameron, 1980; US Department of Transportation, Federal Aviation Administration, 1982, 2008). A “pendulum effect” can result from the envelope being accelerated rapidly downwind with the basket initially lagging. Aeronauts are also careful not to overheat the envelope and exceed envelope’s never-exceed temperature, which may be challenging when launching heavy and/or at high DAs. Additionally, low propane vapor pressure reduces heat generation making launches in windy conditions hazardous. On the other hand, an excessive climb during liftoff must also be avoided for several reasons, one of which is that the parachute vent may open due to excessive dynamic pressure, which would cause significant loss of buoyancy.

The effect of controlling variables on the net aerostatic lift can be assessed from the Eq. (13). A 10% envelope volume decrease due to (strong) wind-induced distortions will cause 10% decrease in the aerostatic net lift. A 10% atmospheric pressure decrease (due to higher elevation) will cause a 10% decrease in the net aerostatic lift. On the other hand, a 5% increase of the ambient air (absolute) temperature will cause about 15–20% decrease of the net aerostatic lift. A 5% decrease of the hot air temperature will cause about 10–15% decrease in the static effective lift. Superheat functions (Daidzic, 2021) for ambient and hot air are computed at given steady-state point.

Two biggest problems that need to be addressed in the future are accurate predictions of the envelope aerodynamic coefficients due to slip flow and the absence of the flight-test data on false-lift launches. The simulations presented show general agreement with the “false-lift” balloon takeoffs experience. More elaborate modelling of envelope deformation, aerodynamic drag coefficients, and heat balance will be conducted in future refinements. Panel methods may be used to estimate aerodynamic coefficient of envelope’s lift and drag. Flight tests of balloon liftoff with strong surface winds are hazardous, expensive, and complex and were never performed before to the best of our knowledge.

Conclusions

A mathematical model of free hot-air balloon launch in windy conditions has been developed. A model is based on the conservation of the linear momentum in horizontal and vertical directions using launch site as the center of the topocentric frame-of-reference. Linear momentum conservation equations represent a set of four non-linear first-order ODEs. Some ODEs could be solved in closed-form, while the Riccati-type equation with variable coefficients for the vertical acceleration was solved using Runge-Kutta ODE solvers. The aerodynamic lift is caused by Venturi-type flow over the top of the balloon envelope causing suction pressure and aerodynamic lift. Aerodynamic drag acts in both lateral and longitudinal directions. Somewhat unexpected is the long duration of the asymptotic horizontal acceleration. It takes 10 half-

times to reach 90.9% of the wind velocity in a step function response. Any change in wind speed and/or direction will thus cause slow response to horizontal wind step inputs. Similar analysis applies to vertical accelerations, i.e., balloon response to thermals and downdrafts. The higher the lateral drag coefficient of the envelope is, the shorter the balloon’s half-times are. A condition for safe launch was developed in terms of the minimum required average envelope temperature for which the net aerostatic lift overcomes inert weight of the balloon. Novel perturbation analysis was presented to highlight the sensitivity of the net aerostatic lift to changes in controlling parameters. An algebraic semi-empirical approach was developed to model and simulate envelope shape distortions and enhanced convective cooling due to slip flow and their combined effect on the net aerostatic buoyancy. Two different cases with surface winds were simulated – with undistorted envelope and with enhanced convective cooling and envelope distortions. Although no access to any experimental or flight test data was available presented results are in good agreement with ballooning practice and experience. Since balloon takeoffs are essentially performed in downwind direction, obstacle clearance becomes an issue. It has been shown that balloons may stop climbing and even start descending shortly after liftoff despite intense heat inputs. Although the presented analysis focuses on manned free hot-air balloons, the aerodynamic considerations can also be applied to manned and unmanned tethered and free gas and hybrid balloon liftoffs.

References

- Aaron, K. M., Heun, M. K., & Nock, K. T. (2002). A method for balloon trajectory control. *Advances in Space Research*, 30(5), 1227–1232. [https://doi.org/10.1016/S0273-1177\(02\)00526-4](https://doi.org/10.1016/S0273-1177(02)00526-4)
- Abell, M. L., & Braselton, J. P. (2010). *Introductory differential equations with boundary value problems* (3rd ed.). Elsevier (Academic Press).
- Anderson, J. D. Jr. (1991). *Fundamentals of aerodynamics* (2nd ed.). McGraw-Hill.
- Cameron, D. (1980). *Ballooning handbook*. Pelham Books (Penguin Group).
- Cameron, J., Smith, I. S., Cutts, J. A., Raque, S., Jones, J., & Wu, J. (1999, 28 June–1 July 1999). Versatile modeling and simulation of Earth and planetary balloon systems. In *AIAA-99-3876, 13th AIAA Lighter-Than-Air Systems Technology Conference*. Norfolk, Virginia. <https://doi.org/10.2514/6.1999-3876>
- Carlson, L. A., & Horn, W. J. (1983). New thermal and trajectory model for high-altitude balloons. *Journal of Aircraft*, 20(6), 500–507. <https://doi.org/10.2514/3.44900>
- Carnahan, B., Luther, H. A., & Wilkes, J. O. (1969). *Applied numerical methods*. John Wiley & Sons.
- Chapra, S. C., & Canale, R. P. (2006). *Numerical methods for engineers* (5th ed.). McGraw-Hill.
- Daidzic, N. E. (2014). Could we colonize Venus? *Professional Pilot*, 48(3), 92–96.
- Daidzic, N. E. (2015). Efficient general computational method for estimation of standard atmosphere parameters. *International Journal of Aviation Aeronautics, and Aerospace*, 2(1), 1–35. <https://doi.org/10.15394/ijaaa.2015.1053>

- Daidzic, N. E. (2021). Mathematical model of hot-air balloon steady-state vertical flight performance. *Aviation*, 25(3), 149–158. <https://doi.org/10.3846/aviation.2021.15330>
- Das, T., Mukherjee R., & Cameron, J. (2003). Optimal trajectory planning for hot-air balloons in linear wind fields. *Journal of Guidance, Control, and Dynamics*, 26(3), 416–424. <https://doi.org/10.2514/2.5079>
- Davis, H. T. (1962). *Introduction to nonlinear differential and integral equations*. Dover.
- Dorrington, G. E. (2013). Buoyancy estimation of a Montgolfière in the atmosphere of Titan. *Aeronautical Journal*, 177(1195), 1–15. <https://doi.org/10.1017/S0001924000008605>
- Du, H., Li, J., Qu, Z., Zhang, L., & Lv, M. 2019. Flight performance simulation and station-keeping endurance analysis for stratospheric super-pressure balloon in real wind field. *Aerospace Science and Technology*, 86, 1–10. <https://doi.org/10.1016/j.ast.2019.01.001>
- Furfaro, R., Lunine, J. I., Elfes, A., & Reh, K. (2008). Wind-based navigation of a hot-air balloon on titan: A feasibility study. In *Proceedings of SPIE – the International Society for Optical Engineering*, 6960. Orlando, FL. <https://doi.org/10.1117/12.777654>
- Granger, R. A. (1995). *Fluid mechanics*. Dover.
- Houghton, E. L., & Carpenter, P. W. (1993). *Aerodynamics for engineering students* (4th ed.). Edward Arnold, Hodder & Stoughton.
- Jackson, D. D. (1980). *The aeronauts*. Time-Life Books.
- Jackson, J. P., & Dichtl, R. J. (1977). *The science and art of hot-air ballooning*. Garland Publishing.
- Kayhan, O., & Hastaoglu, M. A. (2014). Modelling of stratospheric balloon using transport phenomena and gas compress-release system. *Journal of Thermophysics and Heat Transfer*, 28(3), 534–541. <https://doi.org/10.2514/1.T4271>
- Khoury, G. A., & Gillett, J. D. (1999). *Airship technology* (Cambridge Aerospace Series 10). Cambridge University Press.
- Kreider, J. F. (1975). Mathematical modeling of high-altitude balloon performance. In *the 5th Aerodynamic Declaration Systems Conference, AIAA Paper 75-1385*. <https://doi.org/10.2514/6.1975-1385>
- Kreith, F. (1965). *Principles of heat transfer* (2nd. ed). International Textbook Company.
- Kreith, F., & Kreider, J. F. (1974). *Numerical prediction of the performance of high altitude balloons* (NCAR-TN/STR-65 1971, revised 1974). National Center for Atmospheric Research (NCAR).
- Lally, V. E. (1971). *Superpressure balloons for horizontal soundings of the atmosphere* (NCAR-TN-28). National Center for Atmospheric Research (NCAR).
- McCormick, B. W. (1995). *Aerodynamics, aeronautics, and flight mechanics* (2nd ed.). John Wiley & Sons.
- Moran, J. (2003). *An introduction to theoretical and computational aerodynamics*. Dover.
- Morris, A. L. (1975). *Scientific ballooning handbook* (NCAR-TN/IA-99). National Center for Atmospheric Research (NCAR).
- Nayfeh, A. H. (2004). *Perturbation methods*. Wiley-VCH Verlag GmbH & Co. KGaA.
- Press, W. H, Teulkolsky, S. A., Vetterling, W. T., & Flannery, B. P. (1992). *Numerical recipes in FORTRAN: The art of scientific computing* (2nd ed.). University Press.
- Roth, C. H. (1917). *A short course on the theory and operation of the free balloon* (2nd ed.) The Goodyear Tire and Rubber Company.
- Shi, H., Song, B., & Yao, Q. (2009). Thermal performance of stratospheric airships during ascent and descent. *Journal of Thermophysics and Heat Transfer*, 23(4), 816–821. <https://doi.org/10.2514/1.42634>
- Spiegel, M. R. (1981). *Applied differential equations* (3rd ed.). Prentice-Hall.
- Stefan, K. (1979). Performance theory for hot air balloons. *Journal of Aircraft*, 16(8), 539–542. <https://doi.org/10.2514/3.58561>
- Stefan, B. (1997, 3 June–5 June). Theoretical aerodynamics and thermal endurance for a hot air balloon. In *the 12th AIAA Lighter-Than-Air Systems Technology Conference, AIAA-97-1490*. San Francisco, California. <https://doi.org/10.2514/6.1997-1490>
- Taylor, J. A. (2014). *Principles of Aerostatics: The theory of lighter-than-air flight*. CreateSpace Independent Publishing Platform.
- US Department of Transportation, Federal Aviation Administration. (1981). *Balloon safety tips: Powerlines and thunderstorms* (FAA-P-8740-34, AFO-800-0581). FAA. Washington, DC.
- US Department of Transportation, Federal Aviation Administration. (1982). *Balloon safety tips: False lift, shear & rotors* (FAA-P-8740-39, AFO-800-0582). FAA. Washington, DC.
- US Department of Transportation, Federal Aviation Administration. (1996a). *Operations of hot air balloons with airborne heater* (AC 91-71, 6/13/96 AFS-820). FAA. Washington, DC.
- US Department of Transportation, Federal Aviation Administration. (1996b). *Private Pilot Practical Test Standards for Lighter-than-Air* (FAA-S-8081-17). FAA. Washington, DC.
- US Department of Transportation, Federal Aviation Administration. (1997). *Commercial Pilot Practical Test Standards for Lighter-than-Air* (FAA-S-8081-18). FAA. Washington, DC.
- US Department of Transportation, Federal Aviation Administration. (1999). *Part 31, Airworthiness Standards: Manned Free Balloons*. FAA. Washington, DC.
- US Department of Transportation, Federal Aviation Administration. (2008). *Balloon flying handbook* (FAA-H-8083-11A). FAA. Washington, DC.
- Weber, H. J., & Arfken, G. B. (2004). *Essential mathematical methods for physicists*. Elsevier (Academic Press).
- Zwillinger, D. (1992). *Handbook of differential equations* (2nd ed.). Academic Press. <https://doi.org/10.1016/B978-0-12-784391-9.50085-3>

Notations

- A – Area (equatorial cross-sectional);
 C_D – Balloon coefficient-of-drag (z-vertical, x-horizontal);
 C_L – Balloon envelope top coefficient-of-lift;
 C_{vm} – Virtual mass coefficient;
 D – Aerodynamic drag (z-vertical, x-horizontal);
 g – Gravitational acceleration (reference terrestrial);
 h_g – Lifting gas (hot-air in this case) enthalpy;
 H – Altitude (Height);
 HT – Acceleration half-time (time to accelerate to half of sharp wind/gust velocity);
 L_{eff} – Balloon effective or net lift (stat-aerostatic, dyn – aerodynamic);
 m_B – Balloon inert mass;
 m_g – Balloon envelope lifting gas (hot-air in this case);
 m_{LBH} – Balloon total mass (includes inert and lifting-gas masses);
 M_i – Balloon inertial mass (includes inert, lifting-gas or hot-air, and virtual mass);
 p – Pressure (g-gas, a-ambient);
 ρ – Mass density (g-hot-air, a-ambient air, B-inert mass density, i-inertial mass density);

t – Time;
 T – Absolute temperature (g-gas or hot-air, a-ambient air);
 u – Slip-speed;
 v – Balloon speed (z-vertical, x-horizontal);
 V_B – Balloon envelope volume;
 w – Wind speed (horizontal);
 W_B – Balloon inert weight.

Abbreviations

BTU – British Thermal Units;
DA – Density Altitude;
FAA – Federal Aviation Administration (civil aviation authority in USA);
FAI – Fédération Aéronautique Internationale;
HTA – Heavier-than-Air;
IC – Initial Condition(s);
ISA – International Standard Atmosphere;
IVP – Initial Value Problem (Cauchy's problem);
LBG – LTA balloon with lifting gas (gas balloon);
LBH – LTA Balloon with airborne heater (Hot-air balloon);
LTA – Lighter-than-Air;
ODE – Ordinary Differential Equation;
PA – Pressure Altitude;
RK2 – Runge-Kutta ODE numerical method of the 2nd order;
SL – Sea-Level;
STP – Standard Temperature and Pressure.